tocols A and C, and imaging protocols B and D, with respect to ACL degenerated group, were not recognized.

Next, we investigated the extent to which histological changes of the ACL could be discriminated using MRI. The MRI and histological findings of the ACL were compared for 25 knees. Histological examination revealed 12 as normal group and 13 as degenerated group. The concordance rate between histological and MRI findings was 5 of 12 (41.7%) for normal group and 8 of 13 (61.5%) for degenerated group. The concordance rate between surgical and MRI findings was 6 of 6 (100%) for normal group and 15 of 19 (78.9%) for degenerated group. There was a statistically significant difference in the concordance rates between histological, surgical, and MRI findings in normal group ($p<0.05$; Table 6).

Table 3 The concordance rate between surgical and MRI findings of degenerated group (Type II) in RA knees

	Imaging protocol			
	A	B	C	D
Concordance	6	13	5	15
Discordance	13	6	14	4
Concordance rate	6/19	13/19	5/19	15/19

Protocol A vs B: $p<0.05$; protocol A vs C: not significant; protocol C vs D: $p<0.01$; protocol B vs D: not significant

Table 4 Concordance rate between surgical and MRI findings of ruptured group (Type III) in RA knees

	Imaging protocol			
	A	B	C	D
Concordance	1	3	2	5
Discordance	6	4	5	2
Concordance rate	1 of 7	3 of 7	2 of 7	5 of 7

Protocol A vs B: not significant; protocol A vs C: not significant; protocol C vs D: not significant; protocol B vs D: not significant

Table 5 Concordance rate between surgical and MRI findings of absent group (Type IV) in RA knees

	Imaging protocol			
	A	B	C	D
Concordance	4	4	4	4
Discordance	0	0	0	0
Concordance rate	4 of 4	4 of 4	4 of 4	4 of 4

Protocol A vs B: not significant; protocol A vs C: not significant; protocol C vs D: not significant; protocol B vs D: not significant

Discussion

Under several MR imaging protocols in RA knees, we investigated the extent to which the pathological state of the ACL could be accurately ascertained, and sought to demonstrate the value of Gd-enhanced MRI in evaluating the ACL in the RA knee.

In conventional MRI findings, ligament is visualized as a low intensity signal on both T1-weighted and T2-weighted scans. Synovial fluid presents a low-intensity signal on T1-weighted images and a high-intensity signal on T2-weighted images. Synovial proliferation is visualized as a low-intensity signal on T1-weighted images and a high-intensity signal on T2-weighted images [15, 16]. Because synovial fluid accumulation and periligamentous synovial proliferation are common findings in RA knees, it is difficult to discriminate between the proliferating synovium, synovial fluid, and the ligament. This problem can be addressed, however, by the use of Gd-enhanced MRI, which is superior for visualizing proliferating synovium. Since Gd-DTPA is distributed mainly in the extracellular space soon after intravenous injection and accumulated in regions of vascular permeability [17], it readily accumulates in the angiogenesis-rich synovial regions in RA. On T1-weighted images, proliferating synovium is visualized as a high-intensity signal and synovial fluid as a lower intensity signal, providing a distinct contrast between proliferating synovium and synovial fluid, and enabling the accurate evaluation of proliferating synovium.

The results of this study suggest that conventional T1-weighted and T2-weighted sagittal images are useful in the evaluation of ACL in Type I (normal group) and Type IV (absent group); however, the concordance rate

Table 6 Concordance rate between histological, surgical, and MRI findings of the ACL in RA knees. *n.s.* not significant

* $p<0.05$: concordance rate between histological, surgical, and MRI findings in normal group

	MRI findings			
	Normal	Degenerated	Concordance rate (%)	
Histological findings				
Normal	5	7	5 of 12 (41.7)	*
Degenerated	5	8	8 of 13 (54.5)	
Surgical findings				n.s.
Normal	6	0	6 of 6 (100)	
Degenerated	4	15	15 of 19 (78.9)	

between surgical findings and MRI findings significantly improved by additional images of protocols B and D compared with images of protocols A and C in Type II (degenerated group). In RA knees the difference of contrast in ligament and synovium is very important in order to evaluate the degenerated ACL accurately. One of the major causes of degenerated ACL is the invasion of inflamed synovium into the ACL. Under the imaging protocols B and D (Gd-enhanced images), the ligament is of low signal intensity and inflamed proliferative synovium is of high signal intensity, and the difference of the contrast in ligament and synovium is more clearly recognized.

The ACL degeneration may have a significant involvement in joint destruction of the knee; therefore, evaluating the extent of degeneration of the ACL may clinically prove important in determining benefits of synovectomy as a treatment option for RA.

This finding suggests that the effect of Gd-DTPA may be pronounced when evaluating the ACL in the RA knee.

We judged that sagittal images alone do not always facilitate evaluation of the femoral attachment of the ACL for patients with severe synovial proliferation at the femoral attachment. So angled coronal image was newly determined as coronal image, parallel to the ACL.But significant differences between sagittal image and angled coronal image, with respect to overall ACL group, were not recognized. Our present investigation revealed that using Gd-DTPA enhancement allowed more accurate evaluation of the ACL in the RA knee.

In this study we investigated whether MRI could describe the pathological changes of ACL in RA knees. Only 40% of ACL with normal histological finding could be judged as normal by MRI. Pronounced periligamentous synovial proliferation was a feature of these cases, and it was concluded that it might be difficult to accurately evaluate all the characteristics of the ACL using MRI. In other words, in RA knees with severe synovial proliferation, it may be difficult to discriminate the invasive synovium going into the ligament from synovium surrounding the ligament. This may be a limitation of Gd-enhanced MRI at present.

Conclusion

Our investigation showed that with Gd-DTPA-enhanced MRI the degree of synovial proliferation around the ACL and the degree of degeneration of the ACL in the RA knee can be evaluated more significantly than with conventional MRI; however, MRI did not enable changes in the properties of the parenchyma of the ligament to be visualized. Nevertheless, in the clinical setting, the present imaging technique does allow the ligament to be evaluated to a certain degree, and may prove useful in the evaluation of temporal changes in the RA knee, and thereby, in determining the timing of synovectomy or other procedures.

References

1. Ishikawa H, Ohno O, Hirohata K (1984) An electron microscopic study of the synovial-bone junction in rheumatoid arthritis. Rheumatol Int 4:1–8
2. Iwata Y, Mort J, Tateishi H, Lee KR (1997) Macrophage cathepsin L, a factor in the erosion of subchondral bone in rheumatoid arthritis. Arthritis Rheum 40:499–509
3. Alexiades M, Scuderi G, Vigorita V, Scott WN (1989) A histologic study of the posterior cruciate ligament in the arthritic knee. Am J Knee Surg 2:153–159
4. Hodler J, Haghighi P, Trudell D, Resnick D (1992) The cruciate ligament of the knee: correlation between MR appearance and gross and histologic findings in cadaveric specimens. Am J Roentgenol 159:357–360
5. Kursunoglu-Brahme S, Riccio T, Weisman MH (1990) Rheumatoid knee: role of gadopentetate dimeglumine-enhanced MR imaging. Radiology 176:831–835
6. Yamato M, Tamai K, Yamaguchi T, Ohno W (1993) MRI of the knee in rheumatoid arthritis: Gd-DTPA perfusion dynamics. J Comput Assist Tomogr 17:781–785
7. Tamai K, Yamato M, Yamaguchi T, Ohno W (1994) Dynamic magnetic resonance imaging for the evaluation of synovitis in patients with rheumatoid arthritis. Arthritis Rheum 37:1151–1157
8. Bjorkengren AG, Geborek P, Rydholm U (1992) MR imaging of the knee in acute rheumatoid arthritis. Synovial uptake of gadolinium-DOTA. Am J Roentgenol 159:569–571
9. Adam G, Dammer M, Bohndorf K (1991) Rheumatoid arthritis of the knee. Value of gadopentetate dimeglumine-enhanced MR imaging. Am J Roentgenol 156:125–129
10. Konig H, Sieper J, Wolf KJ (1990) Rheumatoid arthritis. Evaluation of hypervascular and fibrous with dynamic MR imaging enhanced with Gd-DTPA. Radiology 176:473–477
11. Arnett FC, Edworthy SM, Bloch DA et al. (1988) The American Rheumatism Association 1987 revised criteria for the classification of rheumatoid arthritis. Arthritis Rheum 33:305–315
12. Nakanishi K, Horibe S, Shiozaki Y, Ishida, T, Narumi Y et al. (1997) MRI of normal anterior cruciate ligament (ACL) and reconstructed ACL: comparison of when the knee is extended with when the knee is flexed. Eur Radiol 7:1020–1024
13. Nittu M, Ikeda K, Itay Y (1998) Slightly flexed knee position within a standard knee coil: MR delineation of the anterior cruciate ligament. Eur Radiol 8:113–115

14. Stabler, Glaser C, Reiser M (2000) Musculoskeletal MR: knee. Eur Radiol 10:230-241
15. Reiser MF, Bongartz GP, Erlemann R et al. (1989) Gadolinium-DTPA in rheumatoid arthritis and related diseases: first results with dynamic resonance imaging. Skeletal Radiol 28:591–597
16. Damadian R (1971) Tumor detection by nuclear magnetic resonance. Science 171:1151–1153
17. Higueras Guerrero V, Torregrosa Andre's A, Marti-Bonmati L, Casillas C, Sanfeliu M (1999) Synovialisation of the torn anterior cruciate ligament of the knee: comparison between magnetic resonance and arthroscopy. Eur Radiol 9:1796–1799

Prevention of the Onset and Progression of Collagen-Induced Arthritis in Rats by the Potent p38 Mitogen-Activated Protein Kinase Inhibitor FR167653

MASATAKA NISHIKAWA, AKIRA MYOUI, TETSUYA TOMITA, KOICHIRO TAKAHI, AKIHIDE NAMPEI, AND HIDEKI YOSHIKAWA

Reprinted from Arthritis & Rheumatism, Vol. 48, No. 9, 2003

ARTHRITIS & RHEUMATISM
Vol. 48, No. 9, September 2003, pp 2670–2681
DOI 10.1002/art.11227

Prevention of the Onset and Progression of Collagen-Induced Arthritis in Rats by the Potent p38 Mitogen-Activated Protein Kinase Inhibitor FR167653

Masataka Nishikawa, Akira Myoui, Tetsuya Tomita, Koichiro Takahi, Akihide Nampei, and Hideki Yoshikawa

Objective. **FR167653 is a potent inhibitor of p38 mitogen-activated protein kinase (MAPK) and inhibits tumor necrosis factor α (TNFα) and interleukin-1β (IL-1β) production in inflammatory cells. In this study we investigated the effect of FR167653 on collagen-induced arthritis (CIA).**

Methods. **Rats with CIA were subcutaneously injected with FR167653 (32 mg/kg/day) starting on the day of the booster injection (day 7) in the prophylactic treatment group and after the onset of arthritis (day 21) in the therapeutic treatment group. Hind-paw swelling, body weight, radiographic and histologic scores, and osteoclast number were evaluated. Cytokine levels in the serum and tissue were assessed by enzyme-linked immunosorbent assays. Flow cytometric analysis of T lymphocytes from bone marrow was performed. The effect of FR167653 on in vitro osteoclast formation induced by soluble receptor activator of nuclear factor κB ligand (sRANKL) and TNFα was examined.**

Results. **Swelling of hind paws and loss of weight occurred in the CIA rats, but this was not evident in the prophylactic treatment group. Therapeutic treatment also significantly reduced paw swelling. The mean radiographic and histologic scores as well as the osteoclast numbers were significantly lower in the treatment group than in the CIA rats without treatment. FR167653 treatment reduced the serum levels of TNFα and IL-1β, lowered the IL-1β concentration in the ankle joints, and decreased the CD4−,CD8a+ T cell population in bone marrow. Furthermore, FR167653 inhibited the osteoclast-like cell differentiation induced by both sRANKL and TNFα in vitro.**

Conclusion. **FR167653 prevents the onset of arthritis in a prophylactic treatment model and suppresses the progression of joint destruction in a therapeutic treatment model, suggesting that p38 MAPK is a potential therapeutic target for rheumatoid arthritis.**

Rheumatoid arthritis (RA) is characterized as a chronic and progressive inflammatory process that leads to systemic immunologic abnormalities of the joints (1). It has been suggested that proinflammatory cytokines such as tumor necrosis factor α (TNFα), interleukin-1β (IL-1β), IL-6, and IL-8, which are linked in a cascade, are important in the etiology of RA (2–5). Histopathologic characterization of bone erosions in patients with RA and in animal models of inflammatory arthritis has provided strong evidence that osteoclasts play an important role in focal, marginal, and subchondral bone loss in inflammatory arthritis (6). Recently, the roles of receptor activator of nuclear factor κB ligand (RANKL), a central regulator of osteoclast recruitment and activation, and TNFα have been shown to be crucial in the pathogenesis of rheumatoid joint destruction (7–11).

Although no conventional medications effectively suppress such joint destruction, TNFα blockers (soluble TNFα receptor fusion protein and TNFα blocking antibody), IL-1 blockers (soluble IL-1 receptor and IL-1 receptor antagonist), and monoclonal antibodies that neutralize IL-6 have all successfully decreased the inten-

Supported in part by grants from the Ministry of Education, Culture, Sports, Science, and Technology of Japan, and the Ministry of Health, Labour and Welfare of Japan.

Masataka Nishikawa, MD, Akira Myoui, MD, PhD, Tetsuya Tomita, MD, PhD, Koichiro Takahi, MD, PhD, Akihide Nampei, MD, Hideki Yoshikawa, MD, PhD: Osaka University Graduate School of Medicine, Osaka, Japan.

Address correspondence and reprint requests to Akira Myoui, MD, PhD, Department of Orthopaedics, Osaka University Graduate School of Medicine 2-2 Yamada-oka, Suita, Osaka 565-0871, Japan. E-mail: myoi@ort.med.osaka-u.ac.jp.

Submitted for publication September 12, 2002; accepted in revised form May 9, 2003.

sity of synovitis and prevented or retarded the progression of cartilage destruction, both in experimental models and in human trials (12–26). However, these protein products are limited, due to host immune response, rebound of symptoms, a short half-life, and cost (27–29).

FR167653 was first discovered as a potent inhibitor of TNFα and IL-1β production in lipopolysaccharide-stimulated human monocytes and phytohemagglutinin-M–stimulated human lymphocytes (30,31). FR167653 inhibits the activation of p38 mitogen-activated protein kinase (MAPK) by suppressing the phosphorylation of p38 MAPK, preferentially in the α isoform, but not in the γ isoform (32–34). In addition, p38 MAPK is involved in production of IL-6 and IL-8 induced by TNFα and IL-1β (1,35).

Collagen-induced arthritis (CIA) is a widely used experimental model of polyarthritis that has many histopathologic features in common with RA. TNFα, IL-1β, IL-6, and IL-8 also play an important role in the pathogenesis of CIA (5,36–39). In this study we subcutaneously injected FR167653 into rats with CIA. This study is the first to demonstrate that this p38 MAPK inhibitor effectively prevents the onset and progression of CIA in rats.

MATERIALS AND METHODS

Materials. FR167653 (Figure 1) was kindly provided by Fujisawa Pharmaceutical (Osaka, Japan). Lewis rats were purchased from Clea Japan (Tokyo, Japan). We used 77 rats in this study, all of which were included in 7 in vivo experiments. Bovine type II collagen was purchased from Cosmo Bio (Tokyo, Japan), and Freund's incomplete adjuvant was purchased from Difco (Detroit, MI).

Induction of CIA in rats. CIA was induced using the modified method described by Trentham et al (40). Briefly, 6-week-old female Lewis rats were immunized intradermally with 0.5 mg of bovine type II collagen, which was dissolved in 0.5 ml of 0.1*M* acetic acid at 4°C and emulsified in 0.5 ml of cold Freund's incomplete adjuvant. On day 7, the rats received an intradermal booster injection of half the volume of the first immunization (41). Onset of arthritis in the ankle joints could usually be visually recognized between days 18 and 21.

Experimental protocol. To investigate whether FR167653 prevents arthritis and suppresses joint destruction in vivo, we developed 2 experimental protocols. In the prophylactic treatment model, 8 rats with CIA were subcutaneously injected with 32 mg/kg of FR167653 in sterilized water (FR167653-treated rats in the prophylactic treatment model; FR167653-P rats) every day starting on the day of the collagen booster injection (day 7). Four normal rats (normal rats in the prophylactic treatment model; normal-P rats) and 6 rats with CIA (untreated CIA rats in the prophylactic treatment model; CIA-P rats) were used as controls. All rats in the prophylactic treatment model were killed on day 35.

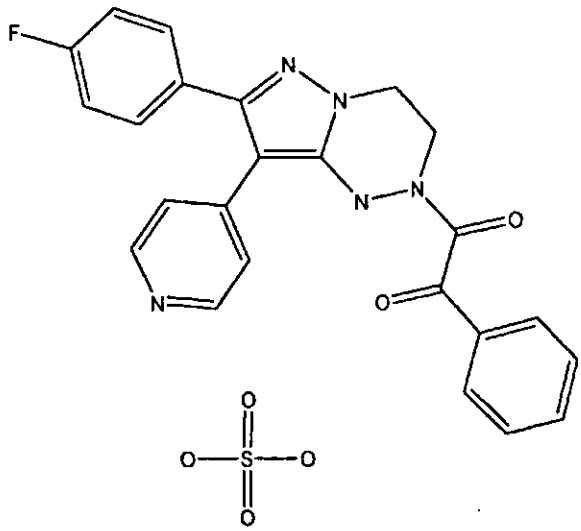

Figure 1. Chemical structure of 1-(7-(4-fluorophenyl)-1,2,3,4-tetrahydro-8-(4-pyridyl)pyrazolo(5,1-c)(1,2,4)triazin-2-yl)-2-phenylethanedione sulfate monohydrate, or FR167653, a p38 mitogen-activated protein kinase inhibitor.

In the therapeutic treatment model, 7 rats with CIA were subcutaneously injected with 32 mg/kg of FR167653 (FR167653-treated rats in the therapeutic model; FR167653-T rats) every day after the onset of arthritis (day 21). Seven rats with CIA (untreated CIA rats in the therapeutic model; CIA-T rats) and 7 normal rats (normal rats in the therapeutic model; normal-T rats) were used as controls. All rats in the therapeutic treatment group were killed on day 49.

Swelling in the hind paws was measured every 7 days using a plethysmometer (model TK-101 CMP; UNICOM, Chiba, Japan). The body weight of rats was also measured every 7 days. All procedures complied with the standards described in the Osaka University Medical School Guidelines for the Care and Use of Laboratory Animals.

Radiologic and histologic studies. At the end of the experiments (day 35 and day 49), the hind paws of rats were imaged on high-speed radiographic film (Fuji Photo Film, Tokyo, Japan), using the MX-20 Specimen Radiography system (Faxitron X-ray, Wheeling, IL). Radiographic scoring criteria were assessed according to the method reported previously (42), on the following scale: 0 = no bone damage, 1 = tissue swelling and edema, 2 = joint erosion, and 3 = bone erosion and osteophyte formation. The ankle joints were fixed in 4% paraformaldehyde, decalcified with EDTA, and embedded in paraffin; 4-μm sections were prepared. The extent of arthritis was assessed according to the method reported previously (43), on sections stained with hematoxylin and eosin, using the following scale: 0 = normal synovium, 1 = synovial membrane hypertrophy and cell infiltrates, 2 = pannus and cartilage erosion, 3 = major erosion of cartilage and subchondral bone, and 4 = loss of joint integrity and ankylosis. The assessment was performed by 2 of the authors (AM and TT),

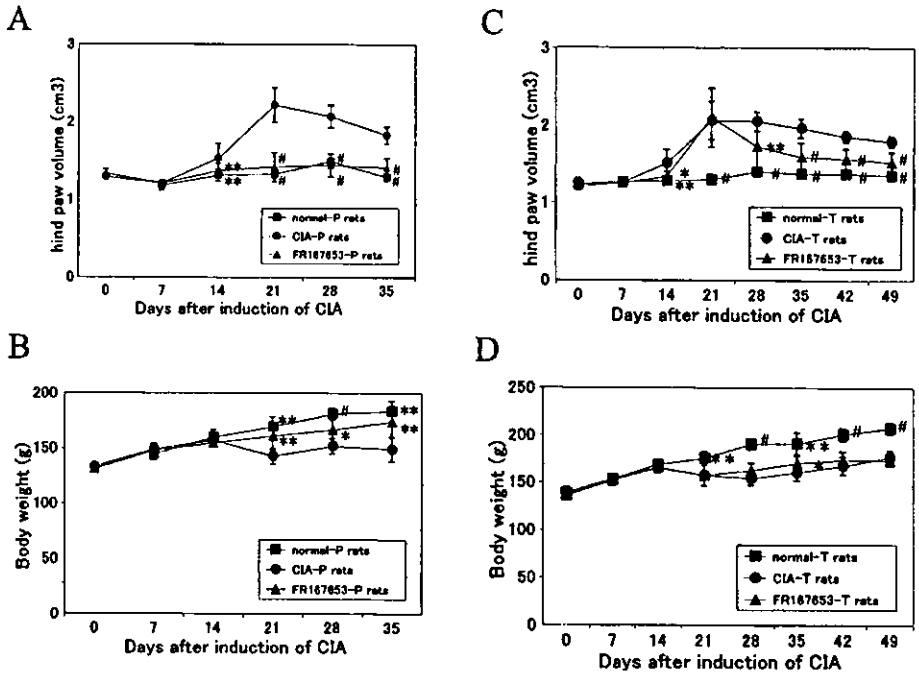

Figure 2. Clinical findings in rats with collagen-induced arthritis (CIA), showing the prophylactic effect (A and B) and therapeutic effect (C and D) of FR167653. A, Maximum paw swelling was observed on day 21 in untreated CIA rats (CIA-P; n = 6), but no increase in paw volume over time was found in CIA rats treated prophylactically with FR167653 (FR167653-P; n = 8). B, An apparent weight loss was seen on day 21 in CIA-P rats compared with FR167653-P rats and normal rats in the prophylactic treatment model (normal-P; n = 4). The weight loss in CIA-P rats continued through day 35. C, Paw swelling in rats treated therapeutically with FR167653 (FR167653-T; n = 7) was significantly less than in untreated CIA rats (CIA-T; n = 7). D, There was no significant weight difference between FR167653-T and CIA-T rats during the entire study period, except for a single time point that showed a marginal difference (day 35). Normal-T = normal rats in the therapeutic treatment model (n = 7). Bars show the mean ± SD. * = $P < 0.05$; ** = $P < 0.01$; # = $P < 0.0001$, versus CIA rats without treatment.

who were blinded to the identity of the specimens, and the average of the 2 scores was used.

To investigate the in vivo activity of osteoclastic bone resorption, sections were stained with a tartrate-resistant acid phosphate (TRAP) staining kit (Hokudo, Sapporo, Japan). The number of osteoclasts, or TRAP-positive multinucleated cells containing 3 or more nuclei, was counted in 10 areas of each ankle (at 200× magnification).

Cytokine level in peripheral blood serum and ankle joints. Peripheral blood samples were collected from rats in the prophylactic model (normal-P, FR167653-P, and CIA-P rats) on day 35. Ankle joints and surrounding tissue (~500 mg, excluding skin) were isolated on day 21 and homogenized with 700 μl of phosphate buffered saline (PBS). After centrifugation, the supernatant was collected from the ankles. The levels of TNFα and IL-1β in the serum and ankle samples were measured with commercial enzyme-linked immunosorbent assay (ELISA) kits (Biosource International, Camarillo, CA). In addition, to investigate whether a humoral response to type II collagen was altered by FR167653 treatment, we also measured serum levels of interferon-γ (IFNγ) and IL-4 using the ELISA kit (Biosource International) in the prophylactic treatment model on day 21. The cytokine concentration in serum and ankle joints was expressed in pg/ml of serum and pg/mg of ankle tissue, respectively. The detection limits of the assay were 15.6 pg/ml for TNFα, 31.2 pg/ml for IL-1β, 21.8 pg/ml for IFNγ, and 7.8 pg/ml for IL-4.

Flow cytometric analysis of bone marrow cells. The effect of FR167653 on the T lymphocyte population was analyzed with bone marrow cells prepared from femurs of rats in the prophylactic treatment model (normal-P, FR167653-P, and CIA-P rats). Cells were collected on day 21 by flushing the bone marrow cavity with minimum essential medium, alpha modification (α-MEM; Invitrogen, Grand Island, NY). After lysing erythrocytes with a lysing buffer (10 m*M* Tris HCl, pH 7.4, 0.83% ammonium chloride), cells were suspended to a concentration of 10^6 cells/ml in PBS containing 0.1% bovine serum albumin. Then, 100 μl of this cell suspension was

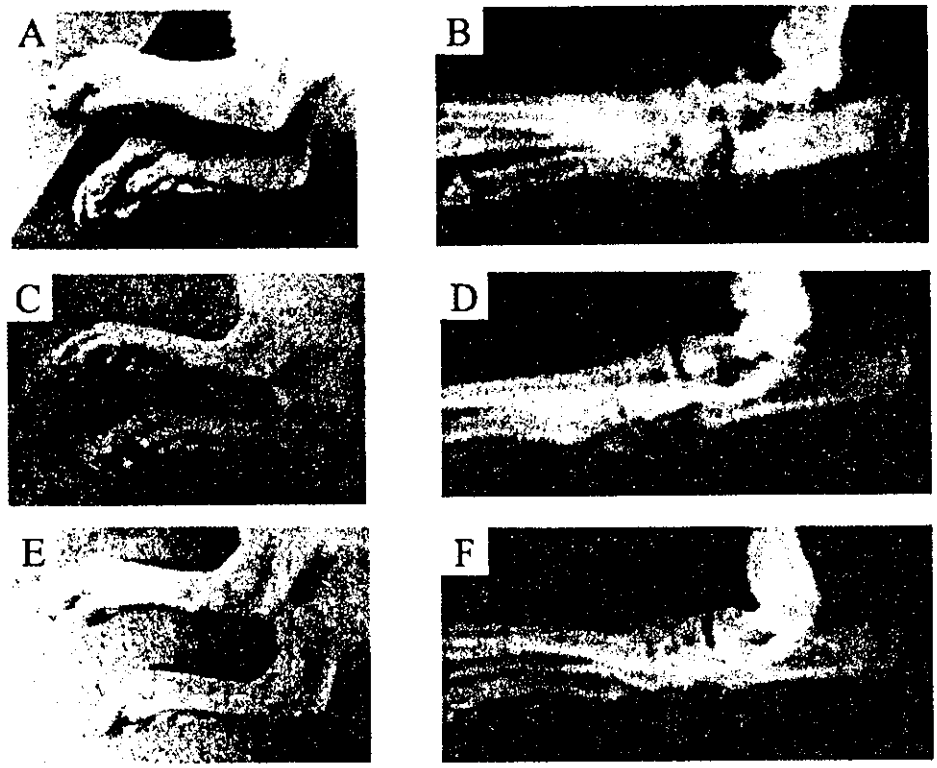

Figure 3. Gross appearance (**A, C,** and **E**) and macroradiographs (**B, D,** and **F**) of rat hind paws in the prophylactic treatment model. Severe paw swelling, bone matrix resorption, and erosion were seen in collagen-induced arthritis (CIA) rats (**A** and **B**), suggesting the presence of active arthritis and joint destruction. When FR167653 was administered prophylactically to CIA rats, those arthritic changes were absent (**C** and **D**). Neither paw swelling nor joint damage were seen in normal rats (**E** and **F**).

exposed to Fc Block (BD PharMingen, San Diego, CA) at 4°C for 5 minutes and stained with fluorescein-conjugated anti-CD4 antibody and phycoerythrin-conjugated anti-CD8a antibody (BD PharMingen) at 4°C for 30 minutes. Two-color flow cytometry was performed using a FACScan (Becton Dickinson, Mountain View, CA) equipped with an argon laser at 488 nm. All specimens were analyzed on the day of collection. To exclude debris or dead cells, the cells were gated on the basis of forward and right angle scatter. Each test used 20,000 cells, and the number of positive cells was expressed as a percentage of the total cell count.

Osteoclast differentiation assay. In vitro osteoclast differentiation induced by macrophage colony-stimulating factor (M-CSF) and soluble RANKL (sRANKL) or TNFα was analyzed using the modified method described by Takeshita et al (44) to investigate the effect of FR167653 on osteoclast formation. After elimination of erythrocytes, bone marrow cells prepared from femurs of 5-week-old female Lewis rats were seeded at 5×10^6 cells per 10-cm petri dish and cultured in α-MEM containing 10% fetal bovine serum (TRACE Scientific, Melbourne, Australia), 1% penicillin/streptomycin (Invitrogen), and 100 ng/ml recombinant human M-CSF (PeproTech EC, London, UK). After 6 days, cells were trypsinized and reseeded at 1×10^4 cells/well in 48-well culture plates in the presence or absence of 100 ng/ml M-CSF, 100 ng/ml recombinant human sRANKL (PeproTech EC), and FR167653, and cultivated for an additional 6 days. Then, cells were washed and stained with the TRAP staining kit.

An in vitro osteoclast formation assay induced by M-CSF and 100 ng/ml murine TNFα (R&D Systems, Minneapolis, MN) was also performed by replacing sRANKL with TNFα in the presence of 200 ng/ml recombinant human osteoprotegerin (Wako Pure Chemical, Osaka, Japan), an endogenous inhibitor of RANKL. Osteoclast-like TRAP-positive multinucleated cells containing 3 or more nuclei were counted. In addition, calcified matrix resorption activity of the osteoclast-like cells was tested using BD BioCoat osteologic calcium hydroxyapatite–coated slides (BD Biosciences, Bedford, MA). At the end of osteoclast formation culture, cells were removed by vigorous washing, and microphotographs (at 100× magnification) of 4 randomly selected fields were taken. The total resorption area on the photographs was calculated by

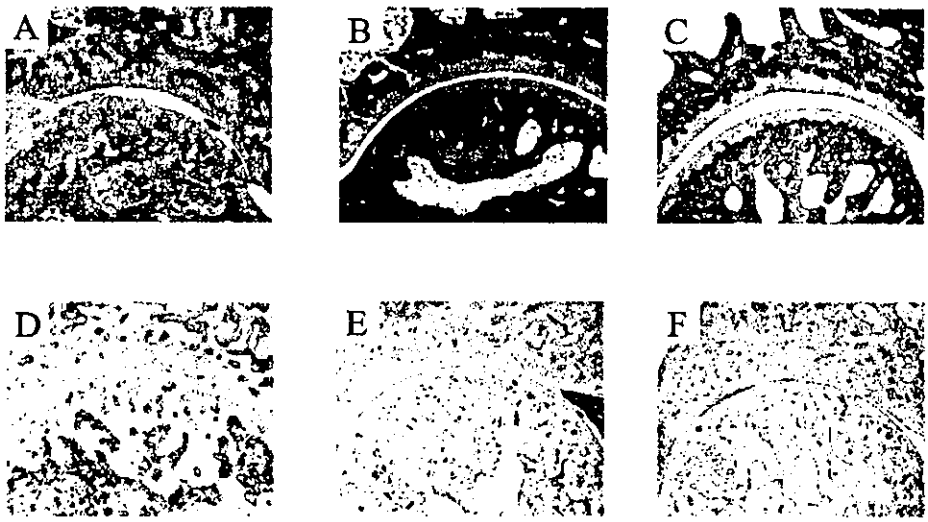

Figure 4. Histologic analysis in the prophylactic treatment model. Histologic features of ankle joints (stained with hematoxylin and eosin in **A–C**; stained with tartrate-resistant acid phosphate [TRAP] in **D–F**) on day 35 in rats in the prophylactic treatment model. **A**, Rats with collagen-induced arthritis (CIA) showed marked infiltration of neutrophils and lymphocytes, with disruption and loss of articular cartilage. **B**, FR167653 prophylactically treated CIA rats showed almost intact articular cartilage and subchondral bone. **C**, Normal rats showed normal articular cartilage and absence of infiltrate in the synovium. **D**, CIA rats showed active periarticular bone resorption with marked infiltration of TRAP-positive osteoclasts. **E**, TRAP-positive multinuclear cell formation was almost completely abolished in FR167653 prophylactically treated CIA rats. **F**, Normal rats showed few TRAP-positive multinuclear cells. (Original magnification × 40.)

using image analysis software, Mac scope version 2.51 (Mitani, Fukui, Japan).

Statistical analysis. Statistical analysis was performed using the unpaired *t* test, Mann-Whitney U test, and analysis of variance with Fisher's protected least significant difference test. Analyses were carried out with STATVIEW, version 4.5 software (SAS Institute, Cary, NC). The statistical significance level was set at a P value of 0.05.

RESULTS

Effect of prophylactic treatment with FR167653 in CIA rats. In the FR167653 prophylactic treatment model, CIA-P rats had maximum paw swelling (mean hind paw volume 2.22 cm^3) by day 21, which gradually reduced after day 21. Most FR167653-P rats showed no paw swelling (mean 1.42 cm^3) on day 21. From day 21 to day 35, the paw volume of the FR167653-P rats was significantly reduced compared with that of the CIA-P rats ($P < 0.0001$) (Figure 2A). The average weight of CIA-P rats on day 21 (142.8 gm) was reduced compared with that of FR167653-P rats (161.1 gm) ($P = 0.0087$). This difference in weight continued through day 35 (CIA-P rats 149.0 gm versus FR167653-P rats 174.1 gm; $P < 0.0039$) (Figure 2B).

Radiographic examination of the hind paws of CIA rats revealed severe bone matrix resorption and erosion that suggested active arthritis and joint destruction. Histologically, CIA rats had severe infiltration of neutrophils, lymphocytes, and TRAP-positive osteoclasts, with disruption and loss of articular cartilage. In the rats prophylactically treated with FR167653 before the onset of arthritis, those radiographic and histologic findings were markedly improved (Figures 3 and 4). The

Table 1. Radiographic score, histologic score, and osteoclast number in the collagen-induced arthritis (CIA) prophylactic treatment model*

Group	No. of joints	Radiographic score	Histologic score	Osteoclast number
FR167653-P rats	16	0.3 ± 0.7†	1.0 ± 0.8†	20.9 ± 38.7‡
CIA-P rats	12	3.0 ± 0.0	3.2 ± 0.5	107.5 ± 55.0
Normal-P rats	8	0.0 ± 0.0†	0.0 ± 0.0§	1.8 ± 2.2‡

* Except where otherwise indicated, values are the mean ± SD. FR167653-P = CIA rats treated prophylactically with FR167653; CIA-P = untreated CIA rats in the prophylactic model; normal-P = normal rats in the prophylactic model.
† $P < 0.0001$ versus CIA-P rats.
‡ $P < 0.01$ versus CIA-P rats.
§ $P = 0.0001$ versus CIA-P rats.

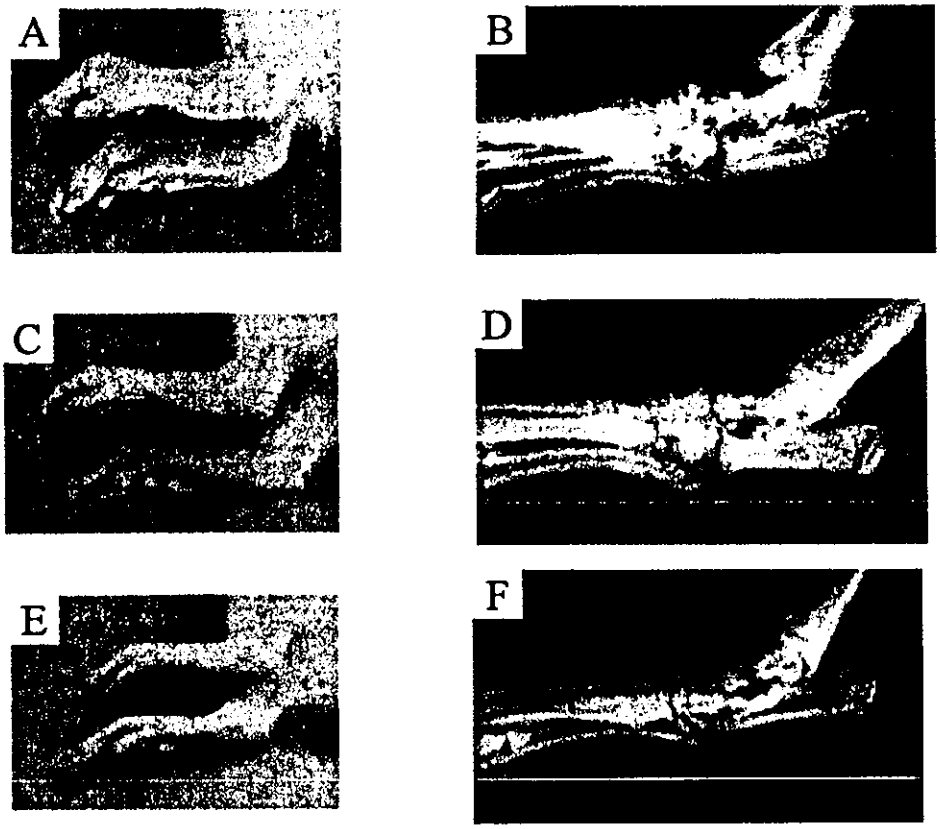

Figure 5. Gross appearance (**A, C,** and **E**) and macroradiographs (**B, D,** and **F**) of rat hind paws in the therapeutic treatment model. Severe paw swelling, bone matrix resorption, and erosion were seen in collagen-induced arthritis (CIA) rats (**A** and **B**), suggesting the presence of active arthritis and joint destruction. When FR167653 was administered therapeutically to rats after the onset of arthritis (**C** and **D**), those arthritic changes were markedly reduced. Neither paw swelling nor joint damage were seen in normal rats (**E** and **F**).

mean radiographic score of 3.0 in CIA-P rats was significantly higher than the mean score of 0.3 in FR167653-P rats and 0.0 in normal-P rats (both $P < 0.0001$ versus CIA-P rats). The mean histologic score of 1.0 in FR167653-P rats was significantly reduced ($P < 0.0001$) compared with the mean score of 3.2 in CIA-P rats. The number of osteoclasts around the ankle joints was significantly fewer in FR167653-P rats (mean 20.9) than in CIA-P rats (mean 107.5) ($P = 0.0002$) (Table 1).

Effect of therapeutic treatment with FR167653 in CIA rats. Although the treatment in the therapeutic model was started after the onset of arthritis, FR167653-T rats had significantly reduced paw swelling (1.73 cm^3 at day 28 and 1.59 cm^3 at day 35) compared with CIA-T rats (2.05 cm^3 at day 28 [$P = 0.0015$] and 1.96 cm^3 at day 35 [$P < 0.0001$]) (Figure 2C). However, there was no statistically significant difference in weight between the FR167653-T rats and CIA-T rats, except at the day 35 time point, which showed a marginal difference ($P = 0.042$) (Figure 2D).

The radiographic severity of joint destruction and histologic findings of abnormalities in the ankle joints of FR167653-T rats were markedly reduced when compared with those in the CIA-T rats (Figures 5 and 6). The mean radiographic and histologic scores in CIA-T rats (2.9 and 3.3, respectively) were significantly higher than those in FR167653-T rats (1.3 and 1.2, respectively) and normal-T rats (0.0 for both) ($P < 0.0001$). The number of osteoclasts around the ankle joints was

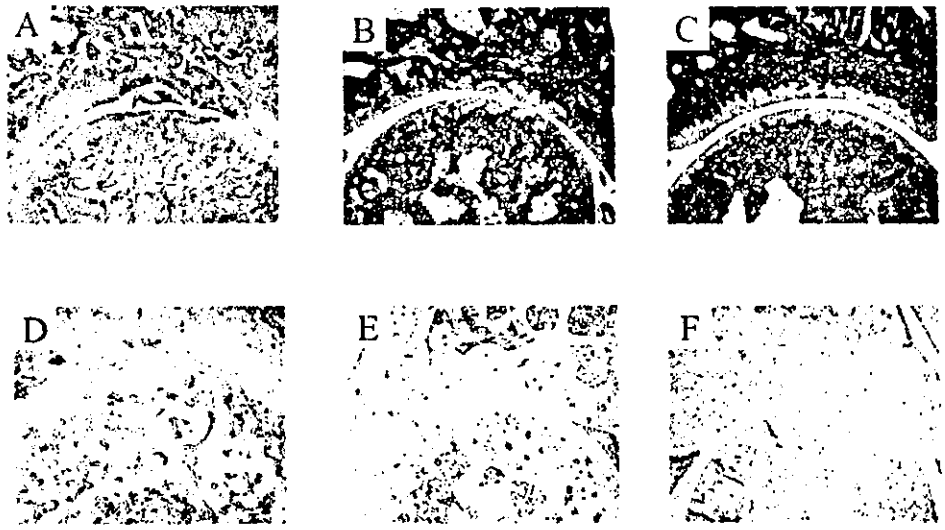

Figure 6. Histologic analysis in the therapeutic treatment model. Histologic features of ankle joints (stained with hematoxylin and eosin in **A–C**; stained with tartrate-resistant acid phosphate [TRAP] in **D–F**) on day 49 in rats in the therapeutic treatment model. **A**, Rats with collagen-induced arthritis (CIA) showed marked infiltration of neutrophils and lymphocytes, with disruption and loss of articular cartilage. **B**, FR167653 therapeutically treated CIA rats showed slight thinning of articular cartilage and intact subchondral bone with mild inflammatory cell infiltration into synovium. **C**, Normal rats showed normal articular cartilage and absence of infiltrate in the synovium. **D**, CIA rats showed active periarticular bone resorption with marked infiltration of TRAP-positive osteoclasts. **E**, TRAP-positive multinuclear cell formation was almost completely abolished in FR167653 therapeutically treated CIA rats. **F**, Normal rats showed few TRAP-positive multinuclear cells. (Original magnification × 40.)

significantly smaller in FR167653-T rats (9.7) than in CIA-T rats (90.0) ($P < 0.0001$) (Table 2).

Cytokine level in peripheral blood serum and ankle joints. The serum concentrations of TNFα (3.16 pg/ml) ($P = 0.0051$) and IL-1β (not detectable) ($P = 0.0041$) in FR167653-P rats were significantly lower than those in CIA-P rats (TNFα 66.7 pg/ml and IL-1β 116.6 pg/ml) (Table 3). The tissue concentration of IL-1β (0.450 pg/mg) ($P < 0.0001$) in the ankle joints of FR167653-P rats was significantly lower than that in CIA-P rats (2.448 pg/mg). However, tissue TNFα levels were similar among the 3 groups (Table 4). IFNγ and IL-4 levels were lower than the detection limit in all groups.

Effect of FR167653 on the T lymphocyte population. The percentages of CD4+,CD8a− and CD4+, CD8a+ T cells in the bone marrow were similar among normal-P, FR167653-P, and CIA-P rats. However, the

Table 2. Radiographic score, histologic score, and osteoclast number in the collagen-induced (CIA) therapeutic treatment model*

Group	No. of joints	Radiographic score	Histologic score	Osteoclast number
FR167653-T rats	10	1.3 ± 0.8†	1.2 ± 0.9‡	9.7 ± 8.9†
CIA-T rats	13	2.9 ± 0.3	3.3 ± 0.6	90.0 ± 44.5
Normal-T rats	14	0.0 ± 0.0†	0.0 ± 0.0†	1.0 ± 1.8†

* Except where otherwise indicated, values are the mean ± SD. FR167653-T = CIA rats treated therapeutically with FR167653; CIA-T = untreated CIA rats in the therapeutic model; normal-T = normal rats in the therapeutic model.
† $P < 0.0001$ versus CIA-T rats.
‡ $P = 0.0001$ versus CIA-T rats.

Table 3. Cytokine levels in the peripheral blood serum in the CIA prophylactic model*

Group	No. of rats	TNFα, pg/ml	IL-1β, pg/ml
FR167653-P rats	5	3.16 ± 7.1†‡	ND†‡
CIA-P rats	6	66.7 ± 25.2	116.6 ± 35.8
Normal-P rats	4	ND†‡	ND†‡

* Except where otherwise indicated, values are the mean ± SD. TNFα = tumor necrosis factor α; IL-1β = interleukin-1β; ND = not detectable (see Table 1 for other definitions).
† $P < 0.01$ versus CIA-P rats.
‡ The values under the detectable limit were treated as 0.0 for statistical analysis.

Table 4. Cytokine levels in the ankle joints in the CIA prophylactic model*

Group	No. of joints	TNFα, pg/mg	IL-1β, pg/mg
FR167653-P rats	6	0.056 ± 0.012	0.450 ± 0.067†
CIA-P rats	6	0.060 ± 0.013	2.448 ± 0.610
Normal-P rats	6	0.052 ± 0.045	0.187 ± 0.090†

* Except where otherwise indicated, values are the mean ± SD. See Tables 1 and 3 for definitions.
† $P < 0.0001$ versus CIA-P rats.

mean percentage of CD4−,CD8a+ T cells in CIA-P rats (16.7%) (Figure 7A) was significantly greater than that in FR167653-P rats (10.6%) ($P = 0.0434$) (Figure 7B) and normal-P rats (8.4%) ($P < 0.006$) (Figure 7C).

Inhibition of osteoclast differentiation and maturation of bone marrow cells induced by M-CSF and sRANKL or TNFα, following treatment with FR167653. In vitro TRAP-positive multinucleated cell formation induced by sRANKL was almost completely abolished by FR167653 ($P < 0.0001$ for all concentrations of FR167653 compared with no FR167653) (Figures 8A and B). FR167653 also inhibited the osteoclast-like cell differentiation induced by TNFα independent of the RANKL/RANK pathway, in a dose-dependent manner ($P < 0.0001$ for all concentrations of FR167653 compared with no FR167653) (Figures 8C and D). Calcified matrix resorption by sRANKL-induced osteoclast-like cells was also inhibited by FR167653 ($P = 0.0433$) (Figure 9).

DISCUSSION

Because p38 MAPK regulates inflammatory cytokines such as TNFα and IL-1β, several researchers have used inhibitors of p38 MAPK in inflammatory disease models in vivo, including adjuvant-induced arthritis, and their results have confirmed the effectiveness of these inhibitors (30–34,45–49). However, the role of p38 MAPK in the CIA model has not been previously investigated. The current study is the first to elucidate the effects of FR167653, a potent p38 MAPK inhibitor, which completely prevented the onset of CIA and also markedly improved the symptoms of inflammatory changes even after the onset of arthritis, with significant reductions in radiographic and histologic degrees of joint injury.

By what mechanism does FR167653 protect the joint against inflammatory injury? There is evidence that the proinflammatory cytokines TNFα and IL-1β help to propagate the extension of a local or systemic inflammatory process. We confirmed that the inflammatory process in the untreated CIA rats led to substantial increases in the serum levels of TNFα and IL-1β and in the ankle-joint concentration of IL-1β. The serum and ankle-joint concentrations of these proinflammatory cytokines were significantly lower in the rats treated prophylactically with FR167653, suggesting that FR167653 inhibits the polyarticular inflammation process and joint destruction by inhibiting the production of TNFα and IL-1β.

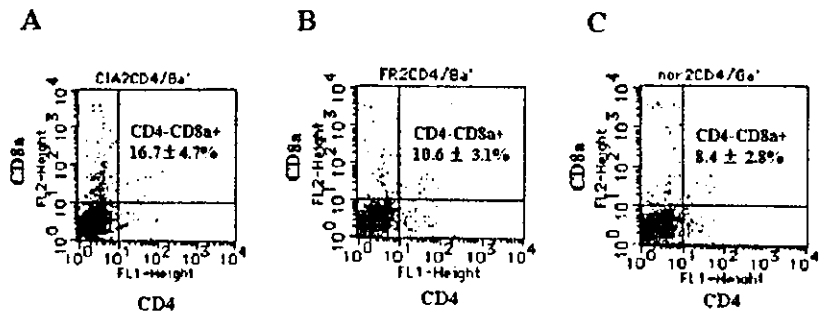

Figure 7. T cell population of bone marrow cells on day 21. Two-color flow cytometric analysis with fluorescein-conjugated anti-CD4 antibody and phycoerythrin-conjugated anti-CD8a antibody was performed using a FACScan equipped with an argon laser at 488 nm on bone marrow cells collected from rats in the prophylactic treatment model. A, Rats with collagen-induced arthritis (CIA). B, FR167653 prophylactically treated CIA rats. C, Normal rats. The proportion of CD4+,CD8a− and CD4+,CD8a+ T cells was similar among the 3 groups of rats. However, the percentage of CD4−,CD8a+ T cells in the untreated CIA rats was significantly greater than that in the FR167653-treated rats and normal rats. Data are the mean ± SD (n = 5).

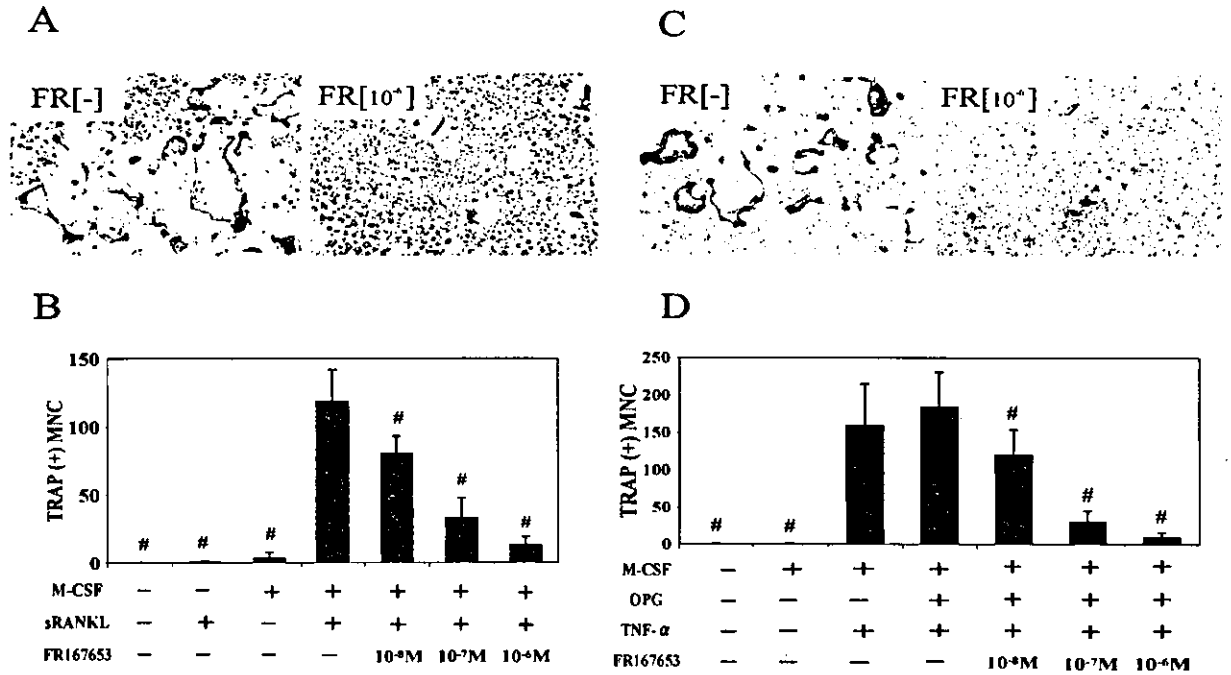

Figure 8. Effect of FR167653 on osteoclast differentiation induced in vitro by macrophage colony-stimulating factor (M-CSF) and soluble receptor activator of nuclear factor κB ligand (sRANKL) or tumor necrosis factor α (TNFα). Rat bone marrow cells were incubated for 6 days in the presence or absence of M-CSF (100 ng/ml), sRANKL (100 ng/ml), and FR167653 ($10^{-8}M$, $10^{-7}M$, or $10^{-6}M$) (A and B) or M-CSF (100 ng/ml), TNFα (100 ng/ml), osteoprotegerin (OPG) (200 ng/ml), and FR167653 ($10^{-8}M$, $10^{-7}M$, or $10^{-6}M$) (C and D). After incubation, cells were stained with the tartrate-resistant acid phosphatase (TRAP) staining kit. Representative microphotographs of TRAP staining induced by M-CSF and sRANKL (A) and by M-CSF, OPG, and TNFα (C) are shown (original magnification × 40). FR[−] = without FR167653; FR[10^{-6}] = with $10^{-6}M$ FR167653. The mean and SD number of TRAP-positive multinuclear cells (MNC) containing 3 or more nuclei is also shown (B and D) (n = 6). # = $P < 0.0001$ versus the M-CSF and sRANKL group in B and versus the M-CSF, OPG, and TNFα group in D.

The involvement of CD8+ T cells in autoimmune disease is multifaceted. CD8+ T cells and major histocompatibility complex class I participate in disease onset in murine and rat autoimmune disease models (50–55). CD8+ T cells may play an important role in initiating CIA (56), but their role is not fully understood (57,58). In the present study, we found a significant increase of CD4−,CD8a+ T cells in the local bone marrow of untreated CIA rats when compared with FR167653-treated rats and normal rats in the prophylactic treatment model. These findings suggest that CD4−,CD8+ T cells play an important role in initiating CIA, and that FR167653 may possibly inhibit the accumulation of inflammation initiators, such as CD4−,CD8a+ T cells, in local bone marrow.

Since macrophage inflammatory protein 1α (MIP-1α) and monocyte chemoattractant protein 1 (MCP-1), which are chemokines that may be responsible for CD8a+ T cell and macrophage infiltration (59,60), are regulated by cytokines such as IL-1α, IL-1β, and TNFα (61), these chemokines may be involved in the mechanism of CD4−,CD8a+ cell accumulation in bone

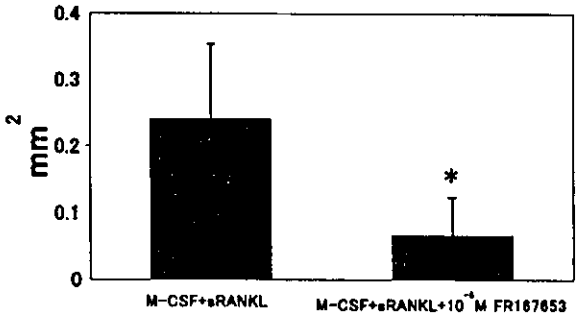

Figure 9. Calcified matrix resorption by osteoclast-like cells, induced by soluble receptor activator of nuclear factor κB ligand (sRANKL). Calcified matrix resorption activity of the osteoclast-like cells was tested using BD BioCoat osteologic calcium hydroxyapatite–coated slides. Rat bone marrow cells were incubated with macrophage colony-stimulating factor (M-CSF; 100 ng/ml) and sRANKL (100 ng/ml) in the presence or absence of FR167653 ($10^{-6}M$). Bars show the mean and SD (n = 4) total resorption area on 4 randomly selected microscopic fields (100× magnification), calculated using an image analysis system. * = $P < 0.05$ versus the M-CSF and sRANKL group.

marrow. Therefore, FR167653 may possibly inhibit cytokines via the inhibition of IL-1β and/or TNFα, resulting in inhibition of inflammatory cell infiltration. However, in our immunohistochemical study, the difference in local expression of MIP-1α and MCP-1 in the periarticular region was marginal between the groups (data not shown).

TNFα and IL-1β are potent inducers of osteoclastic bone resorption. Accordingly, FR167653 inhibition of TNFα and IL-1β production may suppress the periarticular osteolysis in RA. It was recently reported that activation of the p38 MAPK pathway plays an important role in RANKL-induced and TNF-mediated osteoclast differentiation of mouse bone marrow cells (62,63). In the present study, we found that the number of osteoclastic TRAP-positive multinuclear cells in both the prophylactic and therapeutic FR167653-treated rats was significantly smaller than that in their respective untreated CIA groups. Furthermore, in the rat bone marrow culture assay, an FR167653 concentration of $10^{-6}M$ almost completely inhibited the differentiation and maturation of osteoclast-like cells induced by both sRANKL and TNFα. This concentration is equivalent to the serum concentration in rats 8 hours after receiving 32 mg/kg daily by subcutaneous injection (Fujisawa Pharmaceutical: unpublished data). Thus, FR167653 multilaterally inhibits joint destruction by suppressing joint inflammation, reducing serum osteoclastic cytokine levels, and directly inhibiting osteoclast formation and maturation.

In addition to FR167653, other inhibitors of p38 MAPK, SB203580 and SB242235, have been used in several inflammatory disease models, and obvious adverse events were not seen (30–34,45–49). In our in vivo study, we found no adverse events caused by 32 mg/kg/day of FR167653, a dosage that was used in another inflammation model and found to be safe and effective (64). Although most of the in vivo investigations found no adverse effects, one study demonstrated increased plasma creatine levels and lactate dehydrogenase levels in rats (65). The toxicity of FR167653 should be studied extensively.

In conclusion, FR167653, a potent p38 MAPK inhibitor, not only prevents the onset of arthritis by prophylactic treatment, but also suppresses the progression of joint destruction by therapeutic treatment of rats with CIA. FR167653 appears to protect the joints from inflammation injury through the inhibition of TNFα and IL-1β production, recruitment of CD4−,CD8a+ T cells, and osteoclastic bone resorption. These findings suggest that p38 MAPK is a potential therapeutic target for RA.

REFERENCES

1. Suzuki M, Tetsuka T, Yoshida S, Watanabe N, Kobayashi M, Matsui M, et al. The role of p38 mitogen-activated protein kinase in IL-6 and IL-8 production from the TNF-α- or IL-1β-stimulated rheumatoid synovial fibroblast. FEBS Lett 2000;465:23–7.
2. Feldmann M, Brennan FM, Maini RN. Role of cytokines in rheumatoid arthritis. Annu Rev Immunol 1996;14:397–440.
3. Feldmann M, Brennan FM, Maini RN. Rheumatoid arthritis. Cell 1996;85:307–10.
4. Durie FH, Fava RA, Noelle R. Short analytical review: collagen-induced arthritis as a model of rheumatoid arthritis. Clin Immunol Immunopathol 1994;73:11–8.
5. Sasai M, Saeki Y, Ohshima S, Nishioka K, Mima T, Tanaka T, et al. Delayed onset and reduced severity of collagen-induced arthritis in interleukin-6–deficient mice. Arthritis Rheum 1999;42:1635–43.
6. Goldring SR, Gravallese EM. Pathogenesis of bone lesions in rheumatoid arthritis. Curr Rheumatol Rep 2000;4:226–31.
7. Kong YY, Feige U, Sarosi I, Bolon B, Tafuri A, Morony S, et al. Activated T cells regulate bone loss and joint destruction in adjuvant arthritis through osteoprotegerin ligand. Nature 1999;18:304–9.
8. Romas E, Gillespie MT, Martin TJ. Involvement of receptor activator of NFκB ligand and tumor necrosis factor-α in bone destruction in rheumatoid arthritis. Bone 2002;30:340–6.
9. Arend WP, Dayer J-M. Inhibition of the production and effects of interleukin-1 and tumor necrosis factor α in rheumatoid arthritis. Arthritis Rheum 1995;38:151–60.
10. Feldmann M, Elliot MJ, Woody JN, Maini RN. Anti-tumor necrosis factor-α therapy of rheumatoid arthritis. Adv Immunol 1997;64:283–350.
11. Breedveld FC. Future trends in the treatment of rheumatoid arthritis: cytokine targets. Rheumatology 1998;38 Suppl 2:11–3.
12. Brennan FM, Chantry D, Jackson A, Maini R, Feldmann M. Inhibitory effect of TNF alpha antibodies on synovial cell interleukin-1 production in rheumatoid arthritis. Lancet 1989;2:244–7.
13. Wooley PH, Dutcher J, Widmer MB, Gillis S. Influence of a recombinant human soluble tumor necrosis factor receptor FC fusion protein on type II collagen-induced arthritis in mice. J Immunol 1993;151:6602–7.
14. Moreland LW, Baumgartner SW, Schiff MH, Tindall EA, Fleischmann RM, Weaver AL, et al. Treatment of rheumatoid arthritis with a recombinant human necrosis factor receptor (p75)-Fc fusion protein. N Engl J Med 1997;337:141–7.
15. Moreland LW, Schiff MH, Baumgartner SW, Tindall EA, Fleischmann RM, Bulpitt KJ, et al. Etanercept therapy in rheumatoid arthritis: a randomized, controlled trial. Ann Intern Med 1999;130:478–86.
16. Jarvis B, Faulds D. Etanercept: a review of its use in rheumatoid arthritis. Drugs 1999;57:945–66.
17. Moreland LW, Cohen SB, Baumgartner SW, Tindall EA, Bulpitt K, Martin R, et al. Long-term safety and efficacy of etanercept in patients with rheumatoid arthritis. J Rheumatol 2001;28:1238–44.
18. Maini RN, Breedveld FC, Kalden JR, Smolen JS, Davis D, Macfarlane JD, et al. Therapeutic efficacy of multiple intravenous infusions of anti-tumor necrosis factor α monoclonal antibody combined with low-dose weekly methotrexate in rheumatoid arthritis. Arthritis Rheum 1998;41:1552–63.
19. Maini R, St Clair EW, Breedveld F, Furst D, Kalden J, Weisman M, et al. Infliximab (chimeric anti-tumor necrosis factor alpha monoclonal antibody) versus placebo in rheumatoid arthritis patients receiving concomitant methotrexate: a randomised phase III trial. Lancet 1999;354:1932–9.
20. Kavanaugh A, St Clair EW, McCune WJ, Braakman T, Lipsky P. Chimeric anti-tumor necrosis factor-alpha monoclonal antibody treatment of patients with rheumatoid arthritis receiving methotrexate therapy. J Rheumatol 2000;27:841–50.
21. Antoni C, Kalden JR. Combination therapy of the chimeric monoclonal anti-tumor necrosis factor alpha antibody (Infliximab)

with methotrexate in patients with rheumatoid arthritis. Clin Exp Rheumatol 1999;17 Suppl 18:S73–7.
22. Elliott MJ, Maini RN, Feldmann M, Kalden JR, Antoni C, Smolen JS, et al. Randomised double-blind comparison of chimeric monoclonal antibody to tumour necrosis factor α (cA2) versus placebo in rheumatoid arthritis. Lancet 1994;344:1105–10.
23. Arend WP. Interleukin-1 receptor antagonist: discovery, structure and properties. Prog Growth Factor Res 1990;2:193–205.
24. Bendele AM, Chlipala ES, Scherrer J, Frazier J, Sennello G, Rich WJ, et al. Combination benefit of treatment with the cytokine inhibitors interleukin-1 receptor antagonist and PEGylated soluble tumor necrosis factor receptor type I in animal models of rheumatoid arthritis. Arthritis Rheum 2000;43:2648–59.
25. Gabay C, Marinova-Mutafchieva L, Williams RO, Gigley JP, Butler DM, Feldmann M, et al. Increased production of intracellular interleukin-1 receptor antagonist type I in the synovium of mice with collagen-induced arthritis: a possible role in the resolution of arthritis. Arthritis Rheum 2001;44:451–62.
26. Cohen S, Hurd E, Cush J, Schiff M, Weinblatt ME, Moreland LW, et al. Treatment of rheumatoid arthritis with anakinra, a recombinant human interleukin-1 receptor antagonist, in combination with methotrexate: results of a twenty-four–week, multicenter, randomized, double-blind, placebo-controlled trial. Arthritis Rheum 2002;46:614–24.
27. Bemelmans MHA, Gouma DJ, Buurman WA. Influence of nephrectomy on TNF receptor clearance in murine model. J Immunol 1993;150:2007–17.
28. Lipsky PE, Kavanaugh A. The impact of pharmaco-economic considerations on the utilization of novel anti-rheumatic therapies. Rheumatology 1999;38 Suppl 2:41–4.
29. Kalden JR. How do the biologics fit into the current DMARD armamentarium? J Rheumatol 2001;28 Suppl 62:27–35.
30. Yamamoto N, Sakai F, Yamazaki H, Nakahara K, Okuhara M. Effect of FR167653, a cytokine suppressive agent, on endotoxin-induced disseminated intravascular coagulation. Eur J Pharmacol 1996;314:137–42.
31. Yamamoto N, Sakai F, Yamazaki H, Nakahara K, Okuhara M. FR167653, a dual inhibitor of interleukin-1 and tumor necrosis factor-alpha, ameliorates endotoxin-induced shock. Eur J Pharmacol 1997;327:169–75.
32. Takahashi S, Keto Y, Fujita T, Uchiyama T, Yamamoto A. FR167653, a p38 mitogen-activated protein kinase inhibitor, prevents Helicobacter pylori-induced gastritis in Mongolian gerbils. J Pharmacol Exp Ther 2001;296:48–56.
33. Kawashima Y, Takeyoshi I, Otani Y, Koibuchi Y, Yoshinari D, Koyama T, et al. FR167653 attenuates ischemia and reperfusion injury of the rat lung with suppressing p38 mitogen-activated protein kinase. J Heart Lung Transplant 2001;20:568–74.
34. Yoshinari D, Takeyoshi I, Koibuchi Y, Matsumoto K, Kawashima Y, Koyama T, et al. Effects of a dual inhibitor of tumor necrosis factor-α and interleukin-1 on lipopolysaccharide-induced lung injury in rats: involvement of the p38 mitogen-activated protein kinase pathway. Crit Care Med 2001;29:628–34.
35. Miyazawa K, Mori A, Miyata H, Akahane M, Ajisawa Y, Okudaira H. Regulation of interleukin-1-β-induced interleukin-6 gene expression in human fibroblast-like synoviocytes by p38 mitogen-activated protein kinase. J Biol Chem 1998;273:24832–8.
36. Van den Berg WB, Joosten LA, Helsen MM, van de Loo FA. Amelioration of established murine collagen-induced arthritis with anti-IL-1 treatment. Clin Exp Immunol 1994;95:237–43.
37. Joosten LAB, Helsen MMA, van de Loo FAJ, van den Berg WB. Anticytokine treatment of established type II collagen–induced arthritis in DBA/1 mice: a comparative study using anti-TNFα, anti-IL-1α/β, and IL-1Ra. Arthritis Rheum 1996;39:797–809.
38. Mussener A, Litton MJ, Lindroos E, Klareskog L. Cytokine production in synovial tissue of mice with collagen-induced arthritis (CIA). Clin Exp Immunol 1997;107:485–93.
39. Marinova-Mutafchieva L, Williams RO, Mason LJ, Mauri C, Feldmann M, Maini RN. Dynamics of proinflammatory cytokine expression in the joints of mice with collagen-induced arthritis (CIA). Clin Exp Immunol 1997;107:507–12.
40. Trentham D, Townes A, Kang A. Autoimmunity to type II collagen: an experimental model of arthritis. J Exp Med 1977;146: 857–68.
41. Tomita T, Takeuchi E, Tomita N, Morishita R, Kaneko M, Yamamoto K, et al. Suppressed severity of collagen-induced arthritis by in vivo transfection of nuclear factor κB decoy oligodeoxynucleotides as a gene therapy. Arthritis Rheum 1999;42: 2532–42.
42. Cuzzocrea S, Mazzon E, Dugo L, Serraino I, Britti D, De Maio M, et al. Absence of endogenous interleukin-10 enhances the evolution of murine type-II collagen-induced arthritis. Eur Cytokine Netw 2001;12:568–80.
43. Shiozawa S, Shimizu K, Tanaka K, Hino K. Studies on the contribution of c-fos/AP-1 to arthritic joint destruction. J Clin Invest 1997;99:1210–6.
44. Takeshita S, Kaji K, Kudo A. Identification and characterization of the new osteoclast progenitor with macrophage phenotypes being able to differentiate into mature osteoclasts. J Bone Miner Res 2000;15:1477–88.
45. Badger AM, Griswold DE, Kapadia R, Blake S, Swift BA, Hoffman SJ, et al. Disease-modifying activity of SB242235, a selective inhibitor of p38 mitogen-activated protein kinase, in rat adjuvant-induced arthritis. Arthritis Rheum 2000;43:175–83.
46. Shinozaki T, Takagishi K, Tsutsumi S, Yanagawa T, Takeuchi K, Watanabe H, et al. Effect of FR167653, a dual inhibitor of interleukin-1 and tumor necrosis factor, on adjuvant arthritis in rats. Mod Rheumatol 2001;11:300–3.
47. Aiba M, Takeyoshi I, Sunose Y, Iwazaki S, Tsutsumi H, Ohwada S, et al. FR167653 ameliorates pulmonary damage in ischemia-reperfusion injury in a canine lung transplantation model. J Heart Lung Transplant 2000;19:879–86.
48. Kobayashi N, Kataoka T, Ono A, Tsukimi Y, Okabe S. Role of p38 mitogen-activated protein kinase in the healing of gastric ulcers in rats. J Physiol Pharmacol 2001;52:195–210.
49. Kitada H, Sugitani A, Yamamoto H, Otomo N, Okabe Y, Inoue S, et al. Attenuation of renal ischemia-reperfusion injury by FR167653 in dogs. Surgery 2002;131:654–62.
50. Kong YM, Waldmann H, Cobbold S, Giraldo AA, Fuller BE, Simon LL. Pathogenic mechanisms in murine autoimmune thyroiditis: short- and long-term effects of in vivo depletion of CD4+ and CD8+ cells. Clin Exp Immunol 1989;77:428–33.
51. Mozes E, Kohn LD, Hakim F, Singer DS. Resistance of MHC class I-deficient mice to experimental systemic lupus erythematosus. Science 1993;261:91–3.
52. Katz J, Benoist C, Mathis D. Major histocompatibility complex class I molecules are required for the development of insulitis in non-obese diabetic mice. Eur J Immunol 1993;23:3358–60.
53. Serreze DV, Leiter EH, Christianson GJ, Greiner D, Roopenian DC. Major histocompatibility complex class I-deficient NOD-B2mnull mice are diabetes and insulitis resistant. Diabetes 1994; 43:505–9.
54. Wicker LS, Leiter EH, Todd JA, Renjilian RJ, Peterson E, Fischer PA, et al. Beta 2-microglobulin-deficient NOD mice do not develop insulitis or diabetes. Diabetes 1994;43:500–4.
55. Zhang GX, Ma CG, Xiao BG, Bakhiet M, Link H, Olsson T. Depletion of CD8+ T cells suppresses the development of experimental autoimmune myasthenia gravis in Lewis rats. Eur J Immunol 1995;25:1191–8.
56. Tada Y, Ho A, Koh D, Mak TW. Collagen-induced arthritis in CD4- or CD8-deficient mice: CD8+ T cells play a role in initiation and regulate recovery phase of collagen-induced arthritis. J Immunol 1996;156:4520–6.
57. Larsson P, Goldschmidt TJ, Klareskog L, Holmdahl R. Oestrogen-mediated suppression of collagen-induced arthritis in rats: studies on the role of the thymus and peripheral CD8+ T lymphocytes. Scand J Immunol 1989;30:741–7.

58. Ehinger M, Vestberg M, Johnasson ACM, Johanesson M, Svensson A, Holmdahl R. Influence of CD4 or CD8 deficiency on collagen-induced arthritis. Immunology 2001;103:291–300.
59. Moore KJ, Wada T, Barbee SD, Kelley VR. Gene transfer of RANTES elicits autoimmune renal injury in MRL-Fas^{lpr} mice. Kidney Int 1998;53:1631–8.
60. Wada T, Furuichi K, Segawa C, Shimizu M, Sakai N, Takeda S, et al. MIP-1α and MCP-1 contribute to crescents and interstitial lesions in human crescentic glomerulonephritis. Kidney Int 1999; 56:995–1003.
61. Luster AD. Chemokine-chemotactic cytokines that mediate inflammation. N Engl J Med 1998;338:436–45.
62. Matsumoto M, Sudo T, Saito T, Osada H, Tsujimoto M. Involvement of p38 mitogen-activated protein kinase signaling pathway in osteoclastogenesis mediated by receptor activator of NF-κB ligand (RANKL). J Biol Chem 2000;275:31155–61.
63. Matsumoto M, Sudo T, Maruyama M, Osada H, Tsujimoto M. Activation of p38 mitogen-activated protein kinase is crucial in osteoclastogenesis induced by tumor necrosis factor. FEBS Lett 2000;486:23–8.
64. Wada T, Furuichi K, Sakai N, Iwata Y, Yoshimoto K, Shimizu M, et al. A new anti-inflammatory compound, FR167653, ameliorates crescentic glomerulonephritis in Wistar-Kyoto rats. J Am Soc Nephrol 2000;11:1534–41.
65. Gardiner SM, Kemp PA, March JE, Bennett T. Influence of FR 167653, an inhibitor of TNF-alpha and IL-1, on the cardiovascular responses to chronic infusion of lipopolysaccharide in conscious rats. J Cardiovasc Pharmacol 1999;34:64–9.

J Neurosurg (Spine 1) 100:7–12, 2004

Laminoplasty for cervical myelopathy caused by subaxial lesions in rheumatoid arthritis

YOSHIHIRO MUKAI, M.D., NOBORU HOSONO, M.D., HIRONOBU SAKAURA, M.D., TAKAHIRO ISHII, M.D., TSUYOSHI FUCHIYA, M.D., KEIJU FIJIWARA, M.D., TAKESHI FUJI, M.D., AND HIDEKI YOSHIKAWA, M.D.

Department of Orthopedic Surgery, Osaka University Graduate School of Medicine; Department of Orthopedic Surgery, Osaka Prefectural Hospital; and Department of Orthopedic Surgery, Osaka Koseinenkin Hospital, Osaka, Japan

Object. Although controversy exists regarding surgical treatment for rheumatoid subaxial lesions, no detailed studies have been conducted to examine the efficacy of laminoplasty in such cases. To discuss indications for laminoplasty in rheumatoid subaxial lesions, the authors retrospectively investigated clinical and radiological outcomes in patients who underwent laminoplasty for subaxial lesions.

Methods. Thirty patients (11 men and 19 women) underwent laminoplasty for rheumatoid subaxial lesions. The patients were divided into those with mutilating-type rheumatoid arthritis (RA) and those with nonmutilating-type RA according to the number of eroding joints. As of final follow-up examination laminoplasty resulted in improvement of myelopathy in 24 patients (seven with mutilating- and 17 with nonmutilating-type RA) and transient or no improvement in six (five with mutilating- and one with nonmutilating-type RA). In the group with mutilating-type RA, significantly poorer results were displayed ($p < 0.05$). In most patients preoperative radiographs demonstrated vertebral slippage less than or equal to 5 mm at only one or two levels. Postlaminoplasty deterioration of subaxial subluxation and unfavorable alignment change occurred significantly more often in patients with mutilating-type RA ($p < 0.05$).

Conclusions. Patients with nonmutilating-type RA can benefit from laminoplasty for myelopathy due to subaxial lesions.

KEY WORDS • **laminoplasty** • **rheumatoid arthritis** • **subluxation** • **myelopathy**

RHEUMATOID arthritis commonly involves the cervical spine, and instability and neural compression are notorious complications. These disorders occur predominantly in the upper cervical region, where surgical treatments have been well documented.[4,5,16] Conversely, great controversy remains regarding subaxial lesions, such as destruction of facet joints, intervertebral discs, endplates, and spinous processes or inflammatory changes in surrounding soft-tissue support, all of which can lead to hypermobility, subluxation, or step-ladder deformity.[2,3,7,8,14,22,25,26]

Vertebral instability and rheumatoid granulation lead to spinal cord compression. In the subaxial region, relatively minor vertebral translation is more likely to result in spinal cord compression than changes in the upper cervical region, because of the narrowness of the spinal canal. Although multilevel instrumentation-augmented fusion is widely used for subaxial rheumatoid lesions,[20] some authors have reported finding instability at levels adjacent to fused segments.[1,6,7,21] Fusion-related reduced neck mobility can affect swallowing and daily activities in patients with RA.

Laminoplasty was originally indicated for myelopathy due to cervical spondylosis or ossification of the posterior longitudinal ligament, and satisfactory long-term results have been reported.[12,24] We have performed laminoplasty for RA-related subaxial lesions in expectation of preserving cervical ROM and avoiding drawbacks associated with arthrodesis. No detailed study regarding laminoplasty for these lesions has previously been conducted. We retrospectively evaluated clinical and radiological outcomes after performing laminoplasty for subaxial lesions and discuss the indications for this procedure.

Clinical Material and Methods

Patient Population

Between 1990 and 2000, 79 patients with RA underwent surgical intervention for subaxial lesions in our hospitals. Instrumentation-augmented fusion was performed in 47 patients, and the remaining 32 patients underwent laminoplasty. Follow-up data in two patients were insufficient; thus, 30 cases (11 men and 19 women) formed the

Abbreviations used in this paper: RA = rheumatoid arthritis; ROM = range of motion.

basis of this study. Twenty-eight patients underwent C3–7, one patient C4–T1, and one patient C2–5 decompression. This was not a randomized study, and criteria for selecting either laminoplasty or arthrodesis depended on individual surgeons. Laminoplasty was generally indicated in the following cases: 1) when subaxial subluxation was relatively mild and no cervical kyphotic deformity was present; and 2) when the main symptom was myelopathy without significant neck pain. Progressive myelopathy represented the main symptom in all 30 patients. All patients fulfilled established criteria for RA. The mean age of patients at surgery was 63.9 years (range 46–82 years). The mean duration of RA was 16.2 years (range 3–48 years) before surgery.

Each patient was screened for osseous erosion in 68 joints throughout the body by an independent rheumatologist. Patients were divided into two groups according to the number of eroding joints: mutilating-type RA (12 cases), in which more than 40 joints were affected, and nonmutilating-type RA (18 cases), in which 40 or fewer joints were affected.[9,18] In all patients subaxial subluxation of at least 3 mm was present. Concomitant atlantoaxial subluxation and/or vertical subluxation was noted in 21 patients: atlantoaxial subluxation in 10, atlantoaxial subluxation and vertical subluxation in five, and vertical subluxation in six. Two patients had previously undergone upper cervical fusion for the treatment of antlantoaxial subluxation and/or vertical subluxation.

Interventions involved two types of laminoplasty: en bloc procedure[11] in 24 patients and midsagittal splitting procedure[15] in six. En bloc laminoplasty was performed as follows. The spinous processes were removed and bilateral gutters were made at the facet–lamina junctions by using a high-speed drill. On the hinged side, the inner cortex was preserved; on the open side, the inner cortex was completely cut down to the epidural space. The laminae were elevated en bloc, and the removed spinous processes were used as a strut graft to hold the opened laminae. In the midsagittal splitting laminoplasty, the spinous processes were split in the midline by using a high-speed drill, bilateral gutters were made at the facet–lamina junctions, and bone graft was used as a spacer. In most patients autologous bone chip graft was placed on the hinged gutter.

Twenty patients underwent laminoplasty only. Concomitant occiput–C2 or C1–2 fusion was added to laminoplasty in five patients each. In all patients in whom concomitant upper cervical fusion was conducted, the primary myelopathy-inducing lesion was located in the subaxial region. Postoperatively, a cervical collar was routinely worn for 1 month by patients who underwent laminoplasty alone. Patients who underwent concomitant upper cervical fusion were placed in a halo jacket for 1 to 2 months.

Radiographic Evaluation

Consecutive radiographs were examined to determine the number of levels displaying vertebral slippage (≥ 3 mm), extent of slippage, and ROM between C-2 and C-7 on lateral flexion–extension x-ray films. Sagittal cervical alignment on lateral neutral radiographs was classified as lordosis, straight, or kyphosis. All radiographic measurements and classifications were performed by one of the authors in a blinded manner.

Clinical Evaluation

Neurological impairment was evaluated according to the Ranawat classification system[21] (Class I, no neural deficit; Class II, subjective weakness with hyperreflexia and dysesthesia; Class IIIA, objective weakness and long tract signs but ambulating; and Class IIIB, objective weakness and long tract signs but not ambulating). Neck pain was also classified using the Ranawat grading system (0, none; 1, mild; 2, moderate; and 3, severe). The ambulatory ability was classified into four grades (0, can ambulate outdoors without aid; 1, outdoors with aid; 2, indoors; 3, needs a wheelchair; and 4, bedridden). Neurological status was examined just before laminoplasty, 6 months later, and at final follow-up evaluation. For patients who underwent revision surgery, neurological status just before this procedure was used as the final score. The mean postoperative follow-up period was 3.5 years (range 1–9 years).

Statistical Analysis

The chi-square test or Mann–Whitney U-test was used for statistical analysis. Probability values less than 0.05 were considered statistically significant. Analyses were performed using JMP statistical computer software version 5.0 (SAS Institute, Cary, NC).

Results

Radiographic Evaluation

Preoperative dislocation was noted at one level in 22 patients, two levels in five, three levels in two, and four levels in one. Preoperative slippage was 3 to 5 mm in 26 patients and greater than 5 mm in four patients. At final follow up, eight patients (six with mutilating-, two with nonmutilating-type RA) exhibited progression of slippage (Table 1), in two of whom the slippage site displayed spontaneous fusion and stabilization.

Preoperative sagittal cervical alignment was considered lordotic in 17 patients, straight in 11, and kyphotic in only two. Postoperative alignment changes occurred in only five patients (four with mutilating- and one with nonmutilating-type RA). Significant differences in deterioration of

TABLE 1

Correlation between postoperative radiologically documented deterioration and subtype of RA

	RA Type		
	Nonmutilating	Mutilating	p Value*
increase or new development of slippage	2 of 18	6 of 12	<0.05
change of alignment			
lordosis to straight	1	1	<0.05
lordosis to kyphosis		2	
straight to kyphosis		1	

* Statistical analysis according to chi-square test.

TABLE 2

*Summary of clinical data in 30 patients with RA**

Case No.	Age (yrs) at Op, Sex	Postop FU (yrs)	RA Subset	Op	Neurological Deficit Class†			Walking Function Grade		
					Preop	6 Mos	FU	Preop	6 Mos	FU
1	62, F	3.5	NM	EB	IIIA	II	II	3	0	0
2	61, F	1.5	NM	EB & UF	IIIA	II	II	0	0	0
3	55, F	4.5	NM	EB	IIIA	II	II	1	0	0
4	70, F	2.5	NM	EB & UF	IIIA	II	II	2	1	1
5	52, F	3.5	NM	EB	IIIB	IIIA	IIIA	4	2	2
6	67, F	3	NM	MS	IIIB	IIIA	IIIA	4	2	2
7	82, F	1	NM	MS	IIIA	IIIA	IIIA	2	1	1
8	76, F	3	NM	MS	IIIB	IIIA	IIIA	4	3	3
9	72, F	5	NM	MS	IIIA	IIIA	IIIA	3	2	2
10	69, F	4	NM	MS	IIIA	II	II	2	1	1
11	60, M	6	NM	MS & UF	IIIA	II	II	2	0	0
12	47, F	2	NM	EB	IIIA	IIIA	IIIA	2	1	1
13	73, M	6.5	NM	EB & UF	IIIA	II	II	0	0	0
14	66, M	2	NM	EB & UF	IIIA	II	II	2	1	1
15	67, M	2	NM	EB & UF	IIIB	II	II	4	2	2
16	70, F	3	NM	EB	IIIB	IIIA	IIIA	3	2	2
17	75, M	1	NM	EB	IIIA	II	II	0	0	0
18	54, F	9	NM	EB	IIIB	IIIA	IIIB	4	2	3
19	66, M	2	MU	EB & UF	IIIA	II	II	2	1	1
20	64, M	5	MU	EB	IIIB	IIIA	IIIB	3	2	4
21	66, F	3	MU	EB	IIIA	II	II	1	0	0
22	56, M	5	MU	EB	IIIB	IIIB	IIIB	4	4	4
23	70, M	6	MU	EB	IIIB	II	II	3	1	1
24	46, F	2	MU	EB & UF	IIIB	IIIB	IIIB	4	3	4
25	57, F	8	MU	EB	IIIA	II	IIIA	1	1	2
26	62, F	4	MU	EB	IIIB	IIIA	IIIA	3	2	2
27	70, F	1	MU	EB	IIIB	IIIA	IIIA	3	2	2
28	66, M	1	MU	EB	IIIB	IIIA	IIIA	3	1	1
29	61, F	1	MU	EB & UF	IIIA	IIIA	IIIA	3	2	2
30	55, M	3	MU	EB & UF	IIIA	II	IIIB	1	1	4

* EB = en bloc laminoplasty; FU = follow up; MS = midsagittal splitting laminoplasty; MU = mutilating; NM = nonmutilating; UF = upper cervical fusion.

† According to the Ranawat classification system.

subaxial subluxation and alignment change were observed between the two groups (Table 1).

The mean ROM in the sagittal plane between C-2 and C-7 was 29° preoperatively (range 6–63°) and 11.4° postoperatively (range 0–31°). The mean ROM decreased to 39% of its preoperative value following laminoplasty. In five patients no motion was displayed between C-2 and C-7 because spontaneous fusion occurred at all levels after laminoplasty.

Clinical Evaluation

Preoperatively, 14 patients reported no neck pain, 15 experienced moderate (Grade 1, five patients; Grade 2, 10 patients) pain, and only one patient suffered severe (Grade 3) pain. In the 16 patients with preoperative neck pain, 10 indicated pain relief by one or two grades, but the remaining six complained of the same level of pain at final follow up. Postoperative deterioration of neck pain occurred in only one patient.

All 30 patients suffered myelopathy preoperatively: Class IIIA in 17 patients and Class IIIB in 13. Postoperative improvement of at least one Ranawat class occurred in 24 patients, with improvement maintained until final follow up in 20 (Table 2). Although six patients had no neurological improvement in Ranawat class, ability to walk improved postoperatively by at least one grade in five patients, with the improvement maintained until final follow up in four (Table 2).

Of five patients in whom neurological deterioration recurred, in three with mutilating-type RA, significant slippage or vertebral collapse developed; two needed revision surgery comprising occiput–upper thoracic fusion with instrumentation (Fig. 1) and one died suddenly of respiratory dysfunction 2 years after laminoplasty. In the remaining two patients, reasons for deterioration were unknown.

Finally, patients could be divided into two groups based on outcome: Group A (24 cases), in which improvement of myelopathy was demonstrated through final follow up, and Group B (six cases), in which only transient or no improvement of myelopathy occurred. The prevalence of mutilating-type RA was 29.2% in Group A and 83.3% in Group B, representing a significant difference ($p < 0.05$). Preoperative radiological disorders did not significantly affect clinical outcome after laminoplasty (Table 3).

Discussion

Studies of cervical lesions in patients with RA have predominantly focused on the occipitoatlantoaxial complex, whereas subaxial lesions have received less attention. Few detailed descriptions of surgical interventions for subaxial

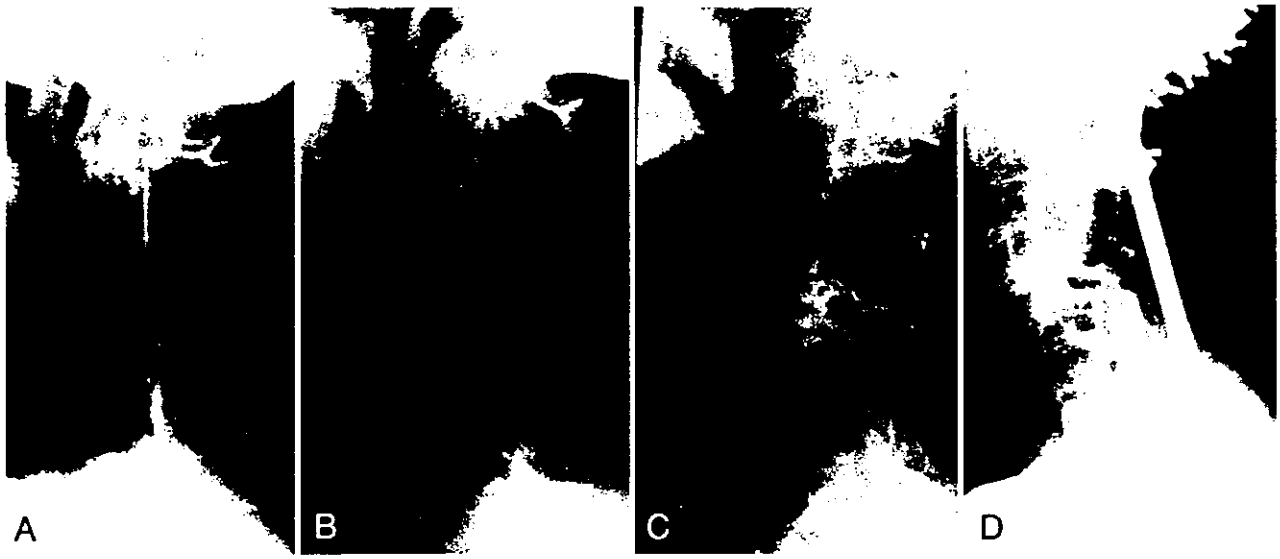

FIG. 1. Lateral radiographs obtained in a 46-year-old woman with mutilating-type RA. A: Preoperative radiograph revealing vertebral slippage at C3–4 in flexion. B: The patient underwent laminoplasty and myelopathy improved from Ranawat Class IIIA to Class II. C: Four years postoperatively, new development of slippage occurred at C4–5 followed by collapse of the C-4 vertebral body. Myelopathy deteriorated to Class IIIB. D: Posterior instrumentation–augmented occiput–T4 fusion was performed. Iliac bone graft was added throughout the instrumentation area. The patient became ambulatory after reoperation.

lesions have been reported. Although laminoplasty has been widely conducted to treat degenerative cervical disease, it has not been generally applied to rheumatoid subaxial lesions because of related postoperative instability and poor results.

Most authors of reports on subaxial lesions have discussed spinal fusion. Ranawat, et al.,[21] reported poor results after anterior spinal fusion for subaxial lesions and recommended posterior fusion. Some authors have insisted that decompression is unnecessary in cases of RA-related myelopathy, as long as solid fusion is attained;[10] however, subaxial compression of the neural elements can also be caused by soft tissues, including pannus formation and extradural rheumatoid nodules. Santavirta, et al.,[23] therefore reported that reduction of subluxation and posterior fusion without laminectomy should be limited to patients in whom signs of cord compression are absent. In their series, vertebral collapse or new subluxations were found at the level adjacent to posterior fusion in some cases, and they indicated the risk of new subluxation below or above the fusion caused by mechanical stress from segmental arthrodesis. Olerud, et al.,[20] have recommended total cervical fusion extending to the upper thoracic spine to avoid complications adjacent to the fused segment.

In the surgical treatment of subaxial lesions, rigid stabilization has been considered crucial, but total cervical fusion would represent overtreatment for subaxial lesions. Based on the belief that some patients with RA harboring subaxial lesions can be successfully managed by undergoing decompression alone without solid fusion, we have performed laminoplasty, a very simple procedure that can preserve mobility of the cervical spine. Compared with laminectomy, kyphotic deformity or malalignment is well known to be reduced following laminoplasty with preservation of posterior structures.[13,17] In the present study, most patients underwent placement of an autologous bone chip graft on the hinged gutter, mainly at the level of subluxation, and we expected local fusion to develop. We anticipated both prevention of cervical instability and preservation of cervical ROM. As a result, cervical ROM was reduced to 39% after laminoplasty. Although some patients indicated complete loss of motion between C-2 and C-7 after laminoplasty, the reasons for such total fusion remain unclear. The quantity of bone graft on the gutter

TABLE 3

*Correlation between preoperative severity of subaxial subluxation and result of laminoplasty**

Variable	Symptomatic Outcome†		p Value
	Group A	Group B	
no. of cases	24	6	
ratio of NM/MU RA cases	17/7	1/5	<0.05‡
no. of levels w/ slippage			
1	18	4	NS§
2	4	1	
3	2		
4		1	
slippage >5 mm	3	1	NS§
alignment			
lordosis	13	4	NS‡
straight	9	2	
kyphosis	2	0	

* NS = not significant.

† Group A, improvement of myelopathy and maintenance after laminoplasty; Group B, only transient or no improvement of myelopathy after laminoplasty.

‡ According to chi-square test.

§ According to Mann–Whitney U-test.